ResearchGate

See discussions, stats, and author profiles for this publication at: https://www.researchgate.net/publication/275722935

Stationary states in gas networks

Article *in* Networks and Heterogeneous Media · June 2015

DOI: 10.3934/nhm.2015.10.295

CITATIONS
2

READS
66

4 authors, including:

Martin Gugat
Friedrich-Alexander-University of Erlangen-N…
108 PUBLICATIONS **953** CITATIONS
SEE PROFILE

Falk Hante
Friedrich-Alexander-University of Erlangen-N…
19 PUBLICATIONS **143** CITATIONS
SEE PROFILE

Günter Leugering
Friedrich-Alexander-University of Erlangen-N…
216 PUBLICATIONS **1,841** CITATIONS
SEE PROFILE

All in-text references underlined in blue are linked to publications on ResearchGate, letting you access and read them immediately.

Available from: Martin Gugat
Retrieved on: 16 September 2016

NETWORKS AND HETEROGENEOUS MEDIA
©American Institute of Mathematical Sciences
Volume **10**, Number **2**, June **2015**
doi:10.3934/nhm.2015.10.295
pp. **295–320**

STATIONARY STATES IN GAS NETWORKS

Martin Gugat, Falk M. Hante
Markus Hirsch-Dick and Günter Leugering

Lehrstuhl Angewandte Mathematik 2
Cauerstr. 11, 91058 Erlangen, Department Mathematik
Friedrich-Alexander Universität Erlangen-Nürnberg (FAU), Germany

(Communicated by Axel Klar)

Abstract. Pipeline networks for gas transportation often contain circles. For such networks it is more difficult to determine the stationary states than for networks without circles. We present a method that allows to compute the stationary states for subsonic pipe flow governed by the isothermal Euler equations for certain pipeline networks that contain circles. We also show that suitably chosen boundary data determine the stationary states uniquely. The construction is based upon novel explicit representations of the stationary states on single pipes for the cases with zero slope and with nonzero slope. In the case with zero slope, the state can be represented using the Lambert–W function.

1. **Introduction.** Essential parts of the transport infrastructure can be modeled as networked systems of hyperbolic balance laws (see [2]). For the management and control of these systems it is important to know the stationary states that exist on the networks.

In this paper, we study pipeline networks for gas transportation. The modeling, analysis and optimal control of gas pipeline networks has been the subject of several studies, for example [6]. As in [6, 12], the flow through each single pipe is modeled by the isothermal Euler equations. An important effect in the pipeline flow is the pressure loss in the gas along the pipe. This effect is modeled by a friction term in the pde that distinguishes this application from the case of conservation laws, that appear for example in the context of traffic flow models (see [10]). For the case without friction, a more general model, the p-system, has been studied in [5] where solutions with bounded total variations are constructed. Also in [18], where numerical models for isothermal junction flow have been studied the friction term does not appear in the balance law. Apart from the friction, the influence of the gravity on the gas flow in the case of non horizontal pipelines is also modeled in the source term. The flow through the pipe junctions in the network is governed by the conservation of mass that yields the Kirchhoff condition and the condition that at the junction in each moment the gas density is the same at all adjacent pipes. The well–posedness of general networked systems of balance laws systems is studied

2010 *Mathematics Subject Classification.* 93C20, 93C15.

Key words and phrases. Network, isothermal Euler equations, stationary state, circles, cycles, gas transportation network.

This work was supported by DFG in the framework of the Collaborative Research Centre CRC/Transregio 154, Mathematical Modelling, Simulation and Optimization Using the Example of Gas Networks, project C03 and project A03 and project A05.

in [19]. Recently, the resilience of natural gas networks during conflicts, crises and disruptions has been studied in [3]. Mixed integer models for the stationary case of gas network optimization have been considered in [17].

For the management of pipeline networks for gas transportation we study stationary solutions in the case of subsonic flow where the absolute value of the velocity of the gas is strictly less than the sound speed in the gas. This is the case that is relevant for gas transportation networks, because if the velocity of the gas in the pipelines is too large, vibrations of the pipes can develop and cause noise pollution. Moreover excessive piping vibration can damage the system. Therefore, there are upper bounds for the velocity of the gas in the operation of gas pipelines. A detailed study of fluid-induced vibration of natural gas pipelines is given in [21]. In the operation of the networks it is desirable to avoid shocks in the gas flow. Therefore we look at classical stationary states.

Due to the friction term, the stationary states are not constant along the pipe except for two cases: The first case is the case of horizontal pipes where the gas is at rest. The second case is the case where the gas flows downhill in the pipe and the gravitational term is in equilibrium with the friction term. It is comparatively simple to construct the stationary states for networks without circles (see [12, 11, 13, 9]) but often the graphs of the pipeline networks contain circles. In this paper we develop a method to construct stationary states for certain networks of this type. Moreover, the construction can also be used to show that the stationary states are uniquely determined by the boundary data.

In our analysis we first look at the stationary states of the governing hyperbolic partial differential equations on a single pipe. We present an explicit representation of the stationary states on each pipe. This result is similar to the representation given in [12] for the case of pipes with zero slope, but even more explicit, since the stationary states is given in terms of a well–known special function, namely the Lambert–W function. Moreover, we also present a representation for pipes with non–zero slope. We show important monotonicity properties of the stationary states with respect to the boundary values, that allow to compute the subsonic classical stationary states on certain gas networks with circles. In addition, we show the uniqueness of the stationary states for suitable boundary data.

This paper is organized as follows. In Section 2 we state the isothermal Euler equations. In Section 3 we consider the stationary states on the edges. We state the differential equations for the density and the squared Mach number. Starting from the discussion of a general class of differential equations in Section 3.1 we derive explicit representations of the stationary states. In Section 3.2 we consider the case of horizontal pipes. Moreover, important monotonicity properties of the stationary states with respect to the boundary data are stated. Using these properties, in Section 4 stationary states on networks are constructed. At the beginning of Section 4 the node conditions that govern the flow through the junctions are stated. In Section 4.1 we consider networks with a finite number of parallel pipes and in Section 4.2 we consider networks that contain a circle with a finite number of parallel chords. In Section 5 an explicit expression for subsonic classical stationary states for a sloped pipe is derived. At the end of the paper conclusions are stated and an outlook is given.

2. The pde-model: A system of balance laws.

Let a graph $G = (V, E)$ of a pipeline network be given. Consider a pipe that corresponds to the edge $e \in$

E. Let $D^e > 0$ denote the diameter, $\lambda^e_{fric}(x) > 0$ the space-dependent Lipschitz continuous friction coefficient and $\alpha^e(x) \in (-\infty, \infty)$ the space-dependent Lipschitz continuous slope. Define $z^e(x) = \sin(\alpha^e(x))$ and $\theta^e(x) = \frac{\lambda^e_{fric}(x)}{D^e}$. Let g denote the gravitational constant and let $a > 0$ denote the sound speed in the gas that we assume to be independent of the pipe. We study the isothermal Euler equations

$$\begin{cases} \rho^e_t + q^e_x = 0, \\ q^e_t + (\frac{(q^e)^2}{\rho^e} + a^2\rho^e)_x = -\frac{1}{2}\theta^e \frac{q^e\,|q^e|}{\rho^e} - \rho^e\, g\, z^e \end{cases}$$

that govern the flow through a single pipe. Here ρ^e denotes the gas density and q^e denotes the flow rate. In our analysis, the velocity $v^e = \frac{q^e}{\rho^e}$ and the Mach number $\frac{v^e}{a}$ will play a central role.

3. **The stationary states on the edges.** Each edge $e \in E$ of the network graph corresponds to an interval of the length $L^e > 0$ with the boundary points $x = 0$ and $x = L^e$. In this section we determine the stationary states on these intervals. The first equation in the isothermal Euler equations implies that for every stationary state, the flow rate q^e is constant. The density ρ^e satisfies an ordinary differential equation on $[0,\, L^e]$ namely

$$\left(\frac{(q^e)^2}{\rho^e} + a^2\rho^e\right)_x = -\frac{1}{2}\theta\,\frac{q^e\,|q^e|}{\rho^e} - \rho^e\, g\, z^e. \tag{1}$$

As stated in the introduction, we consider classical stationary states. Consider the velocity $v^e = \frac{q^e}{\rho^e}$. Define η^e as the square of the Mach number

$$\eta^e = \left(\frac{v^e}{a}\right)^2 = \left(\frac{q^e}{a\,\rho^e}\right)^2. \tag{2}$$

For the subsonic states that are relevant in the applications we have $\eta^e < 1$. Since q^e is constant for stationary states, multiplication of (1) by $\frac{1}{a^2\,\rho^e}$ yields

$$\frac{\rho^e_x}{\rho^e}\left(1 - \left(\frac{q^e}{a\,\rho^e}\right)^2\right) = -\frac{1}{2}\theta\,\mathrm{sign}(q^e)\frac{(q^e)^2}{a^2\,(\rho^e)^2} - \frac{g\,z^e}{a^2}. \tag{3}$$

Hence for the values of η^e for the stationary states we get the ordinary differential equation

$$\eta^e_x = 2\,\frac{\eta^e}{1-\eta^e}\,\left(\frac{1}{2}\,\theta^e\,\mathrm{sign}(q^e)\,\eta^e + \frac{g\,z^e}{a^2}\right). \tag{4}$$

We define

$$c^e_0 = \frac{2\,g\,z^e}{a^2\,\theta^e\,\mathrm{sign}(q^e)}$$

and obtain the ordinary differential equation

$$\eta^e_x = (\theta^e\,\mathrm{sign}(q^e))\;\frac{\eta^e}{1-\eta^e}\;(\,\eta^e + c^e_0)\,. \tag{5}$$

Equation (5) has the constant solution $\eta^e = 0$ and if c^e_0 is constant also the constant solution

$$\eta^e = -c^e_0. \tag{6}$$

In our application, since $\eta^e \geq 0$ this case is only relevant if $c^e_0 < 0$ (that is $\mathrm{sign}(z^e) = -\mathrm{sign}(q^e)$ that is the gas flows downhill).

3.1. **Solutions of a class of differential equations.** The following three lemmas contain results on a general class of ordinary differential equations that have the same structure as the equation (5) for η^e. After the statements and proofs of the Lemmas we will apply them to the case of the isothermal Euler equations.

Lemma 3.1. *Let an interval $I \subset (-\infty, \infty)$ be given. Let the function $F : I \to (-\infty, \infty)$ be continuously differentiable. Assume for all $\tau \in I$ we have $F'(\tau) < 0$ and that $\frac{1}{F'}$ is Lipschitz continuous on I. Let the function $d_0 : (-\infty, \infty) \to (-\infty, \infty)$ be continuous.*

Let $x_0 \in I$ and $\eta_0 \in I$ be given. Consider the differential equation

$$\eta'(x) = -\frac{1}{F'(\eta(x))}\, d_0(x). \tag{7}$$

Then the unique solution η of (7) that satisfies the condition $\eta(x_0) = \eta_0$ is given by

$$\eta(x) = F^{-1}(F(\eta_0) - \int_{x_0}^{x} d_0(s)\, ds) \tag{8}$$

for all $x \in I(x_0, F, d_0) = \{\tau : F(\eta_0) - \int_{x_0}^{\tau} d_0(s)\, ds \in F(I)\}$.

Proof. Since $F'(\tau) < 0$, F is strictly decreasing on I, hence the inverse function F^{-1} is well–defined on $F(I)$. By (8), η is differentiable and the derivative is

$$\eta'(x) = \frac{-d_0(x)}{F'(F^{-1}(F(\eta_0) - \int_{x_0}^{x} d_0(s)\, ds))} = \frac{-d_0(x)}{F'(\eta(x))}.$$

Hence η satisfies (7). Moreover, by (8) we have $\eta(x_0) = F^{-1}(F(\eta_0)) = \eta_0$. The uniqueness of the solution follows by the Picard-Lindelöf theorem. □

Lemma (3.1) allows us to determine the sensitivities of η with respect to η_0. This is stated in the following Lemma.

Lemma 3.2. *For the function $\eta(x)$ given in (8) we have for all $x \in I(x_0, F, d_0)$*

$$\partial_{\eta_0}\eta(x) = \frac{F'(\eta_0)}{F'(\eta(x))} > 0. \tag{9}$$

Thus η is strictly increasing as a function of η_0.

Proof. The definition (8) implies that for the partial derivative we have

$$\partial_{\eta_0}\eta(x) = \frac{F'(\eta_0)}{F'(F^{-1}(F(\eta_0) - \int_{x_0}^{x} d_0(s)\, ds))} = \frac{F'(\eta_0)}{F'(\eta(x))}.$$

Since F' only attains strictly negative values, this implies $\partial_{\eta_0}\eta(x) > 0$. □

If I is a finite interval it can happen that there is a blow-up in $\eta'(x)$ at the boundary of $I(x_0, F, d_0)$ if the derivative of F vanishes at b. First we consider the case that d_0 attains positive values.

Lemma 3.3. *Assume that $I = (a, b]$, F is continuously differentiable on I, $F'(x) < 0$ for all $x \in (a, b)$ and $\lim_{x \to b} F'(x) = 0$. Let $x_0 \in (a, b)$ and $\eta_0 \in (a, b)$ be given.*

Let the function $d_0 : (-\infty, \infty) \to (-\infty, \infty)$ be continuous. If

$$\inf_{x \in (-\infty, \infty)} d_0(x) > 0 \tag{10}$$

define the real number x_c as the unique solution of the equation

$$\int_{x_0}^{x_c} d_0(s)\, ds = F(\eta_0) - F(b). \tag{11}$$

Then $x_0 < x_c$ and for η as defined in (8) we have $\eta(x_c) = b$ and

$$\lim_{x \to x_c} \eta'(x) = \infty, \tag{12}$$

that is at x_c the classical solution of (7) breaks down as x approaches x_c.

Proof. Since $\eta_0 < b$ and F is strictly decreasing we have $F(\eta_0) - F(b) > 0$. Assumption (10) implies that the integral in (11) is strictly increasing to infinity as a function of x_c, hence (11) has a unique solution $x_c > x_0$. Due to (11) we have

$$\eta(x_c) = F^{-1}(F(\eta_0) - \int_{x_0}^{x_c} d_0(s)\, ds) = F^{-1}(F(b)) = b.$$

Using (10) and $-F'(x) = |F'(x)|$ we get

$$\begin{aligned} \lim_{x \to x_c} \eta'(x) &= \lim_{x \to x_c} \frac{-d_0(x)}{F'(\eta(x))} \\ &\geq \inf_{x \in (-\infty, \infty)} d_0(x) \lim_{x \to x_c} \frac{1}{|F'(\eta(x))|} = \infty \end{aligned}$$

and (12) follows. □

If d_0 attains negative values, a different blow up situation occurs: The derivative of η approaches minus infinity, as it is described in Lemma 3.4.

Lemma 3.4. *Assume that $I = (a, b]$, F is continuously differentiable on I, $F'(x) < 0$ for all $x \in (a, b)$ and $\lim_{x \to b} F'(x) = 0$. Let $x_0 \in (a, b)$ and $\eta_0 \in (a, b)$ be given.*

Let the function $d_0 : (-\infty, \infty) \to (-\infty, \infty)$ be continuous. If

$$\sup_{x \in (-\infty, \infty)} d_0(x) < 0 \tag{13}$$

define the real number x_c as the unique solution of the equation (11). Then $x_0 > x_c$ and for η as defined in (8) we have $\eta(x_c) = b$ and

$$\lim_{x \to x_c} \eta'(x) = -\infty, \tag{14}$$

that is at x_c the classical solution of (7) breaks down as x approaches x_c.

The proof is similar to Lemma 3.3.

3.2. **Horizontal pipes.** In this section we study subsonic (that is with $|q^e| < a\, \rho^e$) stationary solutions of the isothermal Euler equation for the flow through horizontal pipes, that is with zero slope $\alpha^e(x) = 0$, hence we have $z^e = 0$. In order to derive an explicit expression, we use the Lambert–W function. For the convenience of the reader, we recall the definition of the Lambert–W function. The Lambert–W function that is also known as product logarithm (see [4, 7, 15, 20]) is the inverse of the map

$$w \mapsto w \exp(w) = z.$$

In our analysis we need the branch $W_{-1}(x)$. This special function is defined as the inverse function of $x \exp(x)$ for $x \in (-\infty, -1)$. Thus $W_{-1}(x) \leq -1$ is defined for $x \in (-\frac{1}{\mathrm{e}}, 0)$. The definition implies $W_{-1}(-1/\mathrm{e}) = -1$ and yields the derivative

$$\frac{d}{dx} W_{-1}(x) = \frac{W_{-1}(x)}{x\,(1 + W_{-1}(x))} < 0. \tag{15}$$

Figure 1 shows a plot of $W_{-1}(x)$.

The following lemma gives the stationary solutions for horizontal pipes.

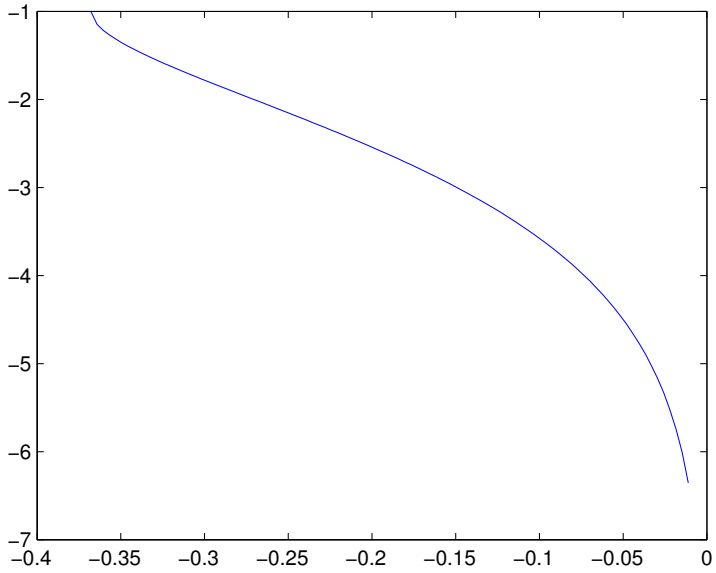

FIGURE 1. The graph of $W_{-1}(x)$ for $x \in [-1/\mathrm{e}, 0)$.

Lemma 3.5. *Assume that $z^e = 0$. Let $x_0 \in [0, L^e]$ be given. Assume that $\eta^e(x_0) < 1$. Then the unique solution of (5) is given by*

$$\eta^e(x) = -\frac{1}{W_{-1}\left(-\exp\left(-(c_1^e - \operatorname{sign}(q^e)\int_{x_0}^x \theta^e(s)\,ds)\right)\right)} \tag{16}$$

with

$$c_1^e = \frac{1}{\eta^e(x_0)} + \ln\left(\eta^e(x_0)\right). \tag{17}$$

For the corresponding density ρ^e that solves the differential equation

$$(\rho^e)_x = \frac{-\frac{1}{2}\theta^e\, q^e\, |q^e|\, \rho^e}{a^2(\rho^e)^2 - (q^e)^2} \tag{18}$$

we have

$$\rho^e(x) = \frac{|q^e|}{a\sqrt{\eta^e(x)}} = \frac{|q^e|}{a}\sqrt{-W_{-1}\left(-\exp\left(-\left(c_1^e - \operatorname{sign}(q^e)\int_{x_0}^x \theta^e(s)\,ds\right)\right)\right)}. \tag{19}$$

Proof. Since the slope is zero, (5) has the form

$$\eta_x^e = \theta^e \operatorname{sign}(q^e)\,\frac{(\eta^e)^2}{1-\eta^e}. \tag{20}$$

Define $d_0(x) = \theta^e \operatorname{sign}(q^e)$ and for $\tau \in (0, 1]$ define

$$F_0(\tau) = \frac{1}{\tau} + \ln(\tau).$$

Then F_0 is differentiable and for the derivative $F_0'(\tau) = \frac{\tau-1}{\tau^2}$ we have $F_0'(\tau) < 0$, thus F_0 is strictly decreasing. The second derivative is $F_0''(\tau) = \frac{2-\tau}{\tau^3}$ and we have $F_0''(\tau) > 0$, thus F_0 is convex. There exists an inverse function F_0^{-1} that is strictly decreasing on the set $(1, \infty)$. The definition of F_0 and d_0 implies that the differential equation (20) has the form of (7). Hence Lemma (3.1) yields the solution in the form (8) where F_0^{-1} appears. The definition of the Lambert–W function implies that for $f \in (1, \infty)$ we have

$$F_0^{-1}(f) = \frac{1}{-W_{-1}(-\exp(-f))}. \tag{21}$$

This can be seen as follows. For $\tau \in (0, 1]$ we have

$$\begin{aligned} \frac{1}{-W_{-1}(-\exp(-F_0(\tau)))} &= \frac{1}{-W_{-1}(-\exp(-\ln(\tau))\,\exp(-\frac{1}{\tau}))} \\ &= \frac{1}{-W_{-1}\left((-\frac{1}{\tau})\,\exp(-\frac{1}{\tau})\right)} = \tau. \end{aligned}$$

Now (8) yields (16) with c_1^e defined by (17). By (2) and (16) we have (19). □

Example 1. For $\lambda_{fric}^e = 0.005$, $D^e = 1$, $q^e = 800$, $\rho^e(0) = 40$, $a = 500$ and $L^e = 100000$ we get the stationary density $\rho^e(x)$ that is shown in Figure 2.

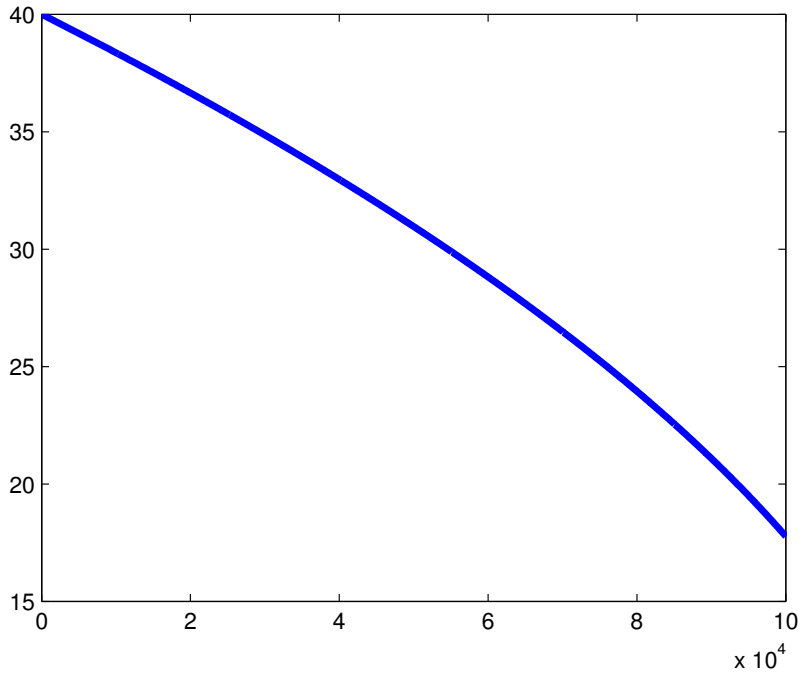

FIGURE 2. The graph of the stationary density $\rho^e(x)$ for $x \in [0, L^e]$ with $z^e = 0$, $\lambda_{fric}^e = 0.005$, $D^e = 1$, $q^e = 800$, $\rho^e(0) = 40$, $a = 500$, $L^e = 10^5$.

Remark 1. In the supersonic case the stationary states can be represented in a similar way using the other branch W_0 of the Lambert–W function.

We introduce the notation

$$\eta(\rho,\, q) = \frac{q^2}{a^2\,\rho^2} \tag{22}$$

and define the function

$$\overline{\rho}^e(\rho,\, q) = \begin{cases} \frac{|q|}{a}\sqrt{-W_{-1}\left(-\frac{1}{\eta(\rho,\,q)}\,\exp\left(-\frac{1}{\eta(\rho,\,q)} + \operatorname{sign}(q)\,\int_0^{L^e}\theta^e(s)\,ds\right)\right)} & \text{if} \quad q \neq 0, \\ \rho & \text{if} \quad q = 0. \end{cases} \tag{23}$$

Then for $x = L^e$ we can write (19) in the form

$$\rho^e(L^e) = \overline{\rho}^e(\rho^e(0),\, q^e). \tag{24}$$

Note that if $q^e > 0$ we have the critical length $x_c > 0$ as defined in (11) with $b = 1$, since $F_0'(1) = 0$. If θ^e is constant we have (as already shown in [12])

$$x_c^e(\eta^e(0)) = \frac{F_0(\eta^e(0)) - 1}{\theta^e}. \tag{25}$$

In general $x_c^e(\eta^e(x_0))$ is determined by the equation

$$\operatorname{sign}(q)\int_{x_0}^{x_c(\eta^e(x_0))}\theta(s)\,ds = F_0(\eta^e(x_0)) - 1 \tag{26}$$

with the choice $x_0 = 0$ if $q^e > 0$ and $x_0 = L^e$ if $q^e < 0$. At $x_c^e(\eta^e(x_0))$ the state becomes sonic, that is the Mach number approaches $b = 1$ and there is a blow up in the derivative ρ_x. Hence at this point the stationary state breaks down as a classical solution. Note that since at the critical length the velocity of the gas approaches the sound speed, it is much to high for the operation of a gas transportation network.

If

$$\operatorname{sign}(q^e)\; L^e < x_c^e(\eta^e(0)) \tag{27}$$

we have the equation

$$\eta^e(L^e) = F_0^{-1}\left(F_0(\eta^e(0)) - \operatorname{sign}(q^e)\int_0^{L^e}\theta^e(s)\,ds\right) \tag{28}$$

and if

$$-\operatorname{sign}(q^e)\; L^e < x_c^e(\eta^e(L^e)) \tag{29}$$

we have

$$\eta^e(0) = F_0^{-1}\left(F_0(\eta^e(L^e)) + \operatorname{sign}(q^e)\int_0^{L^e}\theta^e(s)\,ds\right). \tag{30}$$

Equivalently, if (28) or (30) hold we have

$$F_0(\eta^e(L^e)) = F_0(\eta^e(0)) - \operatorname{sign}(q^e)\int_0^{L^e}\theta^e(s)\,ds. \tag{31}$$

Example 2. For $a = 500$, $q = 800$ and $\rho_0 = 40$, we have $\eta(0) = 1/625$. By (25) this yields the critical length $x_0 = \frac{1}{\theta}617.5622...$ With $\lambda_{fric} = 0.005$, $D = 1$, this yields $x_0 = \frac{D}{\lambda_{fric}}\,617.5622... = 1.2351... * 10^5$.

3.2.1. *Computation of the sensitivities of the stationary states.* In this section we analyze how changes in the boundary data affect the solution. More precisely, we want to know how changes of the boundary data at $x = 0$ affect the values of the solution at the other end $x = L^e$. The following lemma gives the partial derivative of $\rho^e(L^e)$ with respect to $\rho^e(0)$ for a fixed value of q^e. Moreover, we present the partial derivative of $\rho^e(L^e)$ with respect to q^e for a fixed value of $\rho^e(0)$ in the subsonic case with $q^e \neq 0$.

Lemma 3.6. *Assume that a subsonic classical stationary solution exists on* $[0, L^e]$. *For subsonic states with* $q^e \neq 0$ *we have the partial derivatives*

$$\partial_{\rho^e(0)}\rho^e(L^e) = \partial_\rho \overline{\rho}^e(\rho^e(0),\, q^e) = \frac{\rho^e(0)}{\rho^e(L^e)}\,\frac{1-\eta^e(0)}{1-\eta^e(L^e)} > 0, \tag{32}$$

$$\partial_{q^e}\rho^e(L^e) = \partial_q \overline{\rho}^e(\rho^e(0),\, q^e) = -\frac{\rho^e(L^e)}{q^e}\,\frac{\eta^e(L^e)-\eta^e(0)}{\eta^e(0)(1-\eta^e(L^e))} < 0. \tag{33}$$

In particular, $\rho^e(L^e)$ *is strictly increasing as a function of* $\rho^e(0)$ *for a fixed value of* q^e. *Moreover,* $\rho^e(L^e)$ *is strictly decreasing as a function of* q^e.

If $q^e = 0$, *we have* $\rho^e(L^e) = \rho^e(0)$. *Thus for* $q^e = 0$, *we have*

$$\partial_{\rho^e(0)}\rho^e(L^e)|_{q^e=0} = \partial_\rho \overline{\rho}^e(\rho^e(0),\, 0) = 1$$

and also in this case $\rho^e(L^e)$ *is strictly increasing as a function of* $\rho^e(0)$. *We have*

$$\partial_{q^e}\rho^e(L^e)|_{q^e=0} = \partial_q \overline{\rho}^e(\rho^e(0),\, 0) = 0. \tag{34}$$

Proof. Let x and $x_0 \in [0, L^e]$ be given. By (2) we get

$$\partial_{\rho^e(x_0)}\rho^e(x) = \partial_{\rho^e(x_0)}\left(\frac{|q^e|}{a\sqrt{\eta^e(x)}}\right) \tag{35}$$

$$= \frac{|q^e|}{a}\left(-\frac{1}{2}\frac{1}{(\eta^e(x))^{3/2}}\right)\partial_{\eta^e(x_0)}\eta^e(x)\;\partial_{\rho^e(x_0)}\eta^e(x_0). \tag{36}$$

We have $\partial_{\rho^e(x_0)}\eta^e(x_0) = -2\frac{(q^e)^2}{a^2\,\rho^e(x_0)^3}$ and (9) yields

$$\partial_{\eta^e(x_0)}\eta^e(x) = \frac{F_0'(\eta^e(x_0))}{F_0'(\eta^e(x))} \tag{37}$$

$$= \frac{(\eta^e(x))^2}{(\eta^e(x_0))^2}\,\frac{\eta^e(x_0)-1}{\eta^e(x)-1} \tag{38}$$

$$= \frac{(\rho^e(x_0))^4}{(\rho^e(x))^4}\,\frac{\eta^e(x_0)-1}{\eta^e(x)-1}. \tag{39}$$

With the choice $x_0 = 0$ and $x = L^e$ inserting this in (36) yields (32). By (2) we get

$$\partial_{q^e}\rho^e(x) = \partial_{q^e}\left(\frac{|q^e|}{a\sqrt{\eta^e(x)}}\right) \tag{40}$$

$$= \frac{\operatorname{sign}(q^e)}{a\sqrt{\eta^e(x)}} - \frac{|q^e|}{2\,a\,(\eta^e(x))^{3/2}}\,\partial_{\eta^e(x_0)}\eta^e(x)\;\partial_q\eta^e(x_0). \tag{41}$$

We have $\partial_q \eta^e(x_0) = \frac{2\,q^e}{a^2\,\rho^e(x_0)^2}$ and inserting (39) in (41) yields

$$\begin{aligned}\partial_{q^e}\rho^e(x) &= \frac{\rho^e(x)}{q^e} - \frac{a^2(\rho^e(x))^3}{2\,|q^e|^2}\,\frac{(\rho^e(x_0))^4}{(\rho^e(x))^4}\,\frac{\eta^e(x_0)-1}{\eta^e(x)-1}\,\frac{2\,q^e}{a^2\,\rho^e(x_0)^2}\\ &= \frac{\rho^e(x)}{q^e} - \frac{1}{q^e}\,\frac{(\rho^e(x_0))^2}{\rho^e(x)}\,\frac{\eta^e(x_0)-1}{\eta^e(x)-1}.\end{aligned}$$

With the choice $x_0 = 0$ and $x = L^e$ this yields (33).

For $q^e = 0$ we have $\rho^e(L^e) = \rho^e(0)$. By the definition of the partial derivative this yields

$$\begin{aligned}\partial_{q^e}\rho^e(L^e)|_{q^e=0} &= \lim_{q^e\to 0}\frac{\rho^e(L^e)-\rho^e(0)}{q^e}\\ &= \lim_{q^e\to 0}\frac{\int_0^{L^e}(\rho^e)_x(x)\,dx}{q^e}.\end{aligned}$$

From (18) we get

$$\partial_{q^e}\rho^e(L^e)|_{q^e=0} = \lim_{q^e\to 0}|q^e|\int_0^{L^e}\frac{-\frac{1}{2}\theta^e\,\rho^e}{a^2(\rho^e)^2-(q^e)^2}\,dx = 0$$

and (34) follows. □

4. **Stationary states on networks.** In this section we study subsonic stationary states for networks of horizontal pipes. The node conditions that determine the flow dynamics are given in [1] for the case that all pipes have the same diameter D^e.

Let a finite connected directed graph $G = (V, E)$ be given. Each edge $e \in E$ of the graph corresponds to an interval $[0, L^e]$. At the vertices $v \in V$, the flow is governed by the node conditions that require the conservation of mass and the continuity of the density. Let $E_0(v)$ denote the set of edges that are incident to $v \in V$ and $x^e(v) \in \{0, L^e\}$ denote the end of the interval $[0, L^e]$ corresponding to the edge e that is adjacent to v. Define

$$\sigma(e,v) = \begin{cases} -1 & \text{if} \quad x^e(v) = 0 \text{ and } \ e \in E_0(v),\\ 1 & \text{if} \quad x^e(v) = L^e \text{ and } \ e \in E_0(v).\end{cases}$$

Then for all $e, f \in E_0(v)$ continuity of the density means that we have the equation

$$\rho^e(x^e(v)) = \rho^f(x^f(v)). \tag{42}$$

Moreover, we have the Kirchhoff condition

$$\sum_{e\in E_0(v)}\sigma(e,v)\,(D^e)^2\,q^e(x^e(v)) = 0. \tag{43}$$

For networks that do not contain circles, subsonic stationary states can be constructed as follows. Since the Kirchhoff condition is a linear equation for the flow rates, the flow rates of a stationary state can be computed independently of the densities by solving a system of linear equations if the flow rates at all but one at the boundary nodes are given. With our explicit representation (19) for $\rho^e(L^e)$ as a function of $\rho^e(0)$, the flow rate q^e in the pipe and the pipe data, it is easy to compute the corresponding densities of stationary states if the density at one of the boundary nodes of the tree is given. The reason is that if the density at one pipe that is adjacent to a junction is known, by (42) this value determines the density at

FIGURE 3. A graph with two parallel pipes

all adjacent pipes. To obtain a classical stationary state on the network, the length of each pipe where the value of $\eta \in (0, 1)$ at the end point where inflow occurs is given must be less than the corresponding critical length that is defined in (26).

4.1. **Networks with parallel pipes.** First we study the stationary states in a network with two parallel pipes. For our system with $\lambda^e_{fric} > 0$ we give sufficient conditions for the existence of a unique subsonic stationary solution that satisfies the node conditions. By induction we also get the solution for a network with N parallel pipes where N is a natural number.

Let a graph with the structure of Figure 3 be given. We have the set of vertices

$$V = \{a_0, b_0, c_0, d_0\}.$$

Assume that at the first vertex at the left-hand side a_0 the density $\rho_0 > 0$ is given. Moreover, assume that at the last vertex at the right-hand side d_0 the flow rate $q_0 > 0$ is also given and that $D^{(a_0,b_0)} = D^{(c_0,d_0)}$. Assume that the value of the squared Mach number $\eta_0 = \frac{q_0^2}{a^2\,(\rho_0)^2} \in (0, 1)$ is sufficiently small such that for the flow from a_0 to d_0 no blow–up occurs.

Due to the conservation of mass that is (43), at the parallel pipes we have flow rates of the form $q_{red} = \lambda\, q_0\, (D^{(a_0,b_0)})^2/(D^{red})^2$ for the upper parallel edge in Figure 3 and $q_{blue} = (1-\lambda)\, q_0\, (D^{(a_0,b_0)})^2/(D^{blue})^2$ for the lower parallel edge with a real number λ. Here $D^{(a_0,b_0)}$ denotes the diameter of the pipe from a_0 to b_0, D^{red} the diameter of the pipe corresponding to the upper edge and D^{blue} the diameter of the pipe corresponding to the lower edge.

At the edge (a_0, b_0), as in (c_0, d_0), the stationary flow rate is also equal to q_0.

In order to determine the value of λ (that fixes the flow rate in the parallel pipes) we have to take into account the densities at the vertices. The flow rate q_0 at the edge (a_0, b_0) and the density ρ_0 together with the data of the pipe determine the density ρ_1 at the vertex b_0.

At the vertex c_0, a given value of λ determines the densities $\rho_{red}(\lambda)$ at the end of the upper parallel pipe and $\rho_{blue}(1-\lambda)$ at the end of the lower parallel pipe. For a stationary state on the network, the value of λ must be chosen in such a way that these two densities are be equal. Define the auxiliary function

$$d(\lambda) = \rho_{red}(\lambda) - \rho_{blue}(1-\lambda).$$

Then we have $d(0) = \rho_{red}(0) - \rho_{blue}(1)$. For zero flow rate, the density is constant along the pipe, hence $\rho_{red}(0) = \rho_1$. Moreover, due to (18) for positive flow rates the density value is strictly decreasing along the pipe. Hence we have $d(0) = \rho_1 - \rho_{blue}(1) > 0$ and $d(1) = \rho_{red}(1) - \rho_{blue}(0) = \rho_{red}(1) - \rho_1 < 0$. Moreover, the function d is continuous and due to the monotonicity property (33) of ρ presented in Lemma 3.6, it is strictly decreasing. Hence for $|\lambda| > 1$, we have $d(\lambda) \neq 0$ and Bolzano's intermediate value theorem implies that there exists a unique value $\lambda_* \in (0, 1)$ such that $d(\lambda_*) = 0$. This value of λ_* determines uniquely the distribution of the flow rates in the parallel pipes and the density at the vertex c_0. Since on the edge (c_0, d_0)

the flow rate q_0 is known, also the density in d_0 is known. Hence the stationary state on the graph V is uniquely determined by the boundary data ρ_0 and q_0.

Moreover, due to the existence of the partial derivatives with respect to q given in Lemma 3.6, by the implicit function theorem the value of ρ_* at the vertex c_0 is strictly decreasing with respect to q_0 and is continuously differentiable as a function of q_0.

Remark 2. Define $r_{red} = \frac{(D^{(a_0,b_0)})^4}{(D^{red})^4}$ and $r_{blue} = \frac{(D^{(a_0,b_0)})^4}{(D^{blue})^4}$. For $q_0 > 0$, due to (19) the number λ_* is in fact determined by the equation

$$\lambda_*^2\, r_{red} W_{-1}\left(-\frac{1}{\lambda_*^2 r_{red}}\frac{1}{\eta_1}\exp\left(-\frac{1}{\lambda_*^2\, r_{red}}\frac{1}{\eta_1}\right)\ \exp(\int_0^{L_1}\theta_1(s)\,ds)\right)$$

$$= (1-\lambda_*)^2\, r_{blue} W_{-1}\left(-\frac{1}{(1-\lambda_*)^2 r_{blue}}\frac{1}{\eta_1}\exp\left(-\frac{1}{(1-\lambda_*)^2\, r_{blue}}\frac{1}{\eta_1}\right)\ \exp(\int_0^{L_2}\theta_2(s)\,ds)\right)$$

where $\eta_1 = \frac{q_0^2}{a^2\,(\rho_1)^2}$ and $\int_0^{L_1}\theta_1(s)\,ds$ is the value for the upper parallel edge and $\int_0^{L_2}\theta_2(s)\,ds$ is the value for the lower parallel edge.

For the computation of λ_* it is useful to look at the auxiliary function

$$\begin{aligned}
&\alpha(\lambda,\,\eta_1,\,\theta_1,\,L_1,\,\theta_2,\,L_2)\\
=\ &\lambda^2\, r_{red} W_{-1}\left(-\exp\left(-\frac{1}{\eta_1\,\lambda^2\, r_{red}}+\int_0^{L_1}\theta_1(s)\,ds\right)\frac{1}{\eta_1\,\lambda^2\, r_{red}}\right)\\
-\ &(1-\lambda)^2\, r_{blue} W_{-1}\left(-\exp\left(-\frac{1}{\eta_1\,(1-\lambda)^2\, r_{blue}}+\int_0^{L_2}\theta_2(s)\,ds\right)\frac{1}{\eta_1\,(1-\lambda)^2\, r_{blue}}\right)
\end{aligned}$$

since λ_* is the unique root of $\alpha(\cdot,\eta_1,\,\theta_1,\,L_1,\,\theta_2,\,L_2)$.

Example 3. Let $\eta_1 = 1/625$, $\theta_1 = \theta_2 = 0.03$. By (25), the corresponding critical length is $x_0 = 20585.4....$ Let $L_1 = 20000$, $L_2 = 0.5\,L_1$.

Figure 4 shows the graph of α on $(0,1)$ for these parameters with $r_{red} = r_{blue} = 1$.

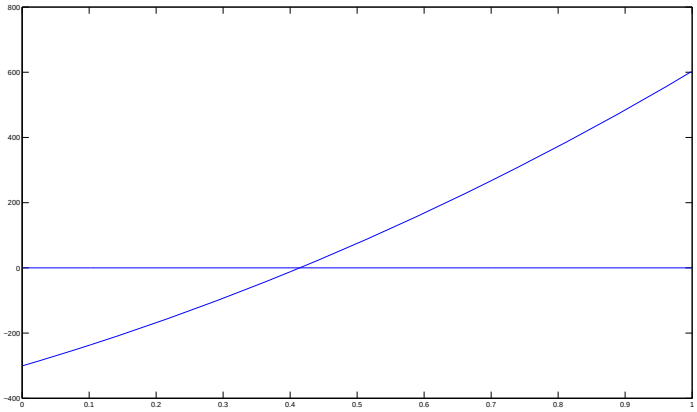

FIGURE 4. The plot of $\alpha(\cdot,\eta_1,\theta_1,L_1,\theta_2,L_2)$ for $x \in [0.001, 0.999]$ and $(\eta_1,\theta_1,L_1,\theta_2,L_2) = (1/625,\ 0.03,\ 20000,\ 0.03,\ 10000)$. The horizontal line is the x-axis.

Example 4. If $\int_0^{L_1} \theta_1(s)\,ds = \int_0^{L_2} \theta_2(s)\,ds$, we have $(\lambda_*)^2\, r_{red} = (1-\lambda_*)^2\, r_{blue}$. If $r_{red} = r_{blue}$ this yields $\lambda_* = \frac{1}{2}$.

Now we consider the more general case of a graph with $N \geq 2$ parallel pipes, where N is a natural number. Figure 5 shows the graph for the case $N = 4$. We show the following result about the corresponding subsonic classical stationary states.

Theorem 4.1. *For a natural number $N \geq 2$ let a network with N horizontal parallel pipes of the type shown in Figure 5 with the corresponding pipe data (lengths and values of θ^e) be given be given. Let the density $\rho_0 > 0$ at a_0 and the flow rate $q_0 > 0$ at d_0 be given. Assume that $\rho_0 > 0$ is sufficiently large in the sense that for the squared Mach number we have*

$$\eta_0 = \frac{q_0^2}{a^2(\rho_0)^2} < 1$$

and the length L_0 of (a_0, b_0) satisfies $L_0 < x_c^{(a_0,b_0)}(\eta_0)$, with $x_c^{(a_0,b_0)}(\eta_0)$ as defined in (26).

Assume that for each of the N parallel pipes, the corresponding length L_i ($i \in \{1, ..., N\}$) is less than the corresponding critical length as defined in (26) with the squared Mach number $\eta_1 = \frac{q_0^2}{a^2(\rho_1)^2}$, where ρ_1 is the value at the vertex b_0. Moreover, assume that also the length of (c_0, d_0) is sufficiently short to allow for a classical subsonic stationary state.

Then on the network there exists a unique classical subsonic stationary state with constant flow rates along each pipe that satisfies (18) on each pipe and the node conditions (42), (43) at the junctions b_0 and c_0.

The common density at the vertex c_0 is continuously differentiable as a function of q_0 and is strictly decreasing with respect to q_0.

Proof. For $N = 2$, we have proved the assertion in the discussion at the beginning of the section. Now we consider a graph with $N \geq 3$ parallel pipes. Then the flow rates at the i-th parallel pipe has the form $q_i = \lambda_i\, q_0\, \frac{(D^{(a_0,b_0)})^2}{D_i^2}$, where $\sum_{i=1}^N \lambda_i = 1$. Note that we have

$$\sum_{i=1}^{N-1} \lambda_i = 1 - \lambda_N.$$

For our proof by induction we assume that for a graph with $N-1$ parallel pipes, for any inflow $\tilde{q}$ at b_0 and density ρ_0 at b_0 there is a uniquely determined distribution $(\lambda_1, ..., \lambda_{N-1})$ to the pipes. This distribution determines the corresponding stationary state and depends continuously on $\tilde{q}$. The common density at the vertex c_0 is continuously differentiable as a function of $\tilde{q}$ and is strictly decreasing with respect to $\tilde{q}$.

This implies that for any choice of λ_N, we can determine $(\lambda_1, ..., \lambda_{N-1})$ such that they generate a stationary state for the flow rate $\tilde{q} = (1-\lambda_N)\, q_0$. This determines uniquely a density $\tilde{\rho}\,(1-\lambda_N)$ at c_0 that corresponds to the value for the $N-1$ first pipes. Similar as in the first step, we can consider the auxiliary function

$$h(\lambda_N) = \rho_N(\lambda_N) - \tilde{\rho}(1-\lambda_N).$$

Then as $d(\lambda)$ in the step for $N = 2$, the function h is strictly decreasing and continuous and we have $h(0) = \rho_1 - \tilde{\rho}(1) > 0$ and $h(1) = \rho_N(1) - \rho_1 < 0$. Now again

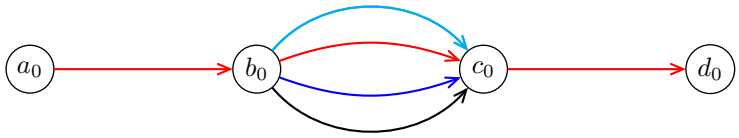

FIGURE 5. A graph with four parallel pipes

Bolzano's intermediate value Theorem implies that there exists a unique value $\lambda_* \in (0,1)$ such that $h(\lambda_*) = 0$. Then the unique stationary state is determined by the flow rates $q_N = \lambda_N\, q_0\, \frac{(D^{(a_0,b_0)})^2}{D_N^2} = \lambda_*\, q_0\, \frac{(D^{(a_0,b_0)})^2}{D_N^2}$ and $(\lambda_1, ..., \lambda_{N-1})$ are uniquely determined as the stationary state for $N-1$ pipes with the flow rate $(1-\lambda_*)q_0$ at b_0. The common density at the vertex c_0 is equal to $\rho_N(\lambda_N) = \tilde{\rho}(1-\lambda_N)$.

Thus by induction, we have shown that for any natural number N, for N parallel pipes we get a unique subsonic stationary state by suitable boundary data q_0 and ρ_0 and that the common density at the vertex c_0 is continuously differentiable as a function of q_0 and is strictly decreasing with respect to q_0. □

4.2. **Networks with a circle with parallel chords.** In this section we want to consider more complicated networks where in particular the direction of flow is not clear a priori. For this purpose, we consider the graph depicted in Figure 6 that contains a circle with the chord e_4. The sign of the flow rate q^{e_4} is not obvious, it can be positive, negative or zero depending on the system data.

Assume that at the first vertex at the left-hand side a_0 the density $\rho_0 > 0$ is known. Moreover, assume that at the last vertex at the right-hand side d_0 the flow rate $q_0 > 0$ is known. We have the set of vertices

$$V = \{a_0,\, b_0,\, c_0,\, d_0,\, e_0,\, f_0\}.$$

We want to show that if ρ_0 is sufficiently large there exists a classical subsonic stationary state that satisfies the node conditions at the junctions.

Note that for the graph that is obtained if one of the five edges

$$(b_0, e_0), (e_0, c_0), (e_0, f_0), (b_0, f_0), (f_0, c_0)$$

is taken away from the graph in this example, the question of existence of a unique stationary state has already been solved in the last section.

As indicated in Figure 6, for the seven edges of the graph, we introduce the notation $e_1 = (a_0, b_0)$, $e_2 = (b_0, e_0)$, $e_3 = (b_0, f_0)$, $e_4 = (e_0, f_0)$, $e_5 = (e_0, c_0)$, $e_6 = (f_0, c_0)$, $e_7 = (c_0, d_0)$. Hence we have the set of edges $E = \{e_1,\, e_2,\, e_3,\, e_4,\, e_5,\, e_6,\, e_7\}$.

For $i \in \{1, 2, 3, 4, 5, 6, 7\}$, let q_i denote the constant flow rate on the edge e_i. Let Q denote the set of all flow rates $(q_i)_i$ that satisfy the imposed boundary conditions and for which the Kirchhoff node conditions (43) are satisfied for all $v \in V$. In this section we assume that all the pipes have the same diameter, hence the factors $(D^e)^2$ can be omitted from (43). Hence the set Q is the solution set of the linear equation

$$M \begin{pmatrix} q_1 \\ q_2 \\ q_3 \\ q_4 \\ q_5 \\ q_6 \\ q_7 \end{pmatrix} = \begin{pmatrix} -q_0 \\ 0 \\ 0 \\ 0 \\ 0 \\ 0 \end{pmatrix} =: b(q_0)$$

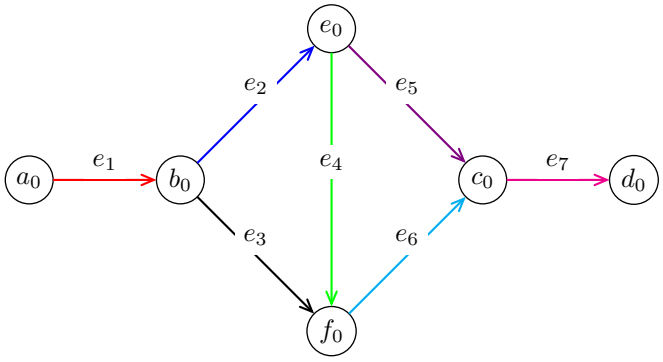

FIGURE 6. A diamond graph

with the matrix $M = \begin{pmatrix} -1 & 0 & 0 & 0 & 0 & 0 & 0 \\ 1 & -1 & -1 & 0 & 0 & 0 & 0 \\ 0 & 1 & 0 & -1 & -1 & 0 & 0 \\ 0 & 0 & 1 & 1 & 0 & -1 & 0 \\ 0 & 0 & 0 & 0 & 1 & 1 & -1 \end{pmatrix}$.

Since M has rank 5, the kernel of M has dimension 2. We have the representation

$$Q = \begin{pmatrix} q_0 \\ q_0 \\ 0 \\ 0 \\ q_0 \\ 0 \\ q_0 \end{pmatrix} + \operatorname{span} \left\{ \begin{pmatrix} 0 \\ 1 \\ -1 \\ 1 \\ 0 \\ 0 \\ 0 \end{pmatrix}, \begin{pmatrix} 0 \\ 0 \\ 0 \\ 1 \\ -1 \\ 1 \\ 0 \end{pmatrix} \right\}.$$

Let us first look at the case where $q_0 = 0$. Then for $q_k = 0$ ($k \in \{1, 2, 3, 4, 5, 6, 7\}$) the density is constant along the pipes and thus with $\rho^v = \rho_0$ for all $v \in V$ we obtain a subsonic stationary state that satisfies the node conditions on the network. Moreover, it is the unique stationary solution for $q_0 = 0$. This can be seen as follows. Suppose that we have a nonzero flow. Then the structure of Q implies that the flow is given by nontrivial a linear combination of the two basis vectors of the kernel of M that appear in the definition of Q. In the network, such a linear combination corresponds to a nonzero circular flow. However, this leads to a contradiction to (42), since in the direction of flow the density values are strictly decreasing along the pipes.

The following lemma states that the function $\overline{\rho}$ defined in (23) is continuous with respect to q at $q = 0$ and states that in the subsonic case the partial derivatives of $\bar{\rho}$ with respect to q and ρ are continuous at $q = 0$.

Lemma 4.2. *We have*

$$\lim_{q \to 0} \overline{\rho}^e(\rho, q) = \rho = \overline{\rho}^e(\rho, 0). \tag{44}$$

The partial derivatives of the map $(\rho, q) \mapsto \overline{\rho}^e(\rho, q)$ exist in a neighborhood of $(\rho_0, 0)$ and we have

$$\lim_{q\to 0} \partial_\rho \overline{\rho}^e(\rho_0,\, q) \;=\; 1 = \partial_\rho \overline{\rho}^e(\rho_0,\, 0), \tag{45}$$

$$\lim_{q\to 0} \partial_q \overline{\rho}^e(\rho_0,\, q) \;=\; 0 = \partial_q \overline{\rho}^e(\rho_0,\, 0). \tag{46}$$

Proof. We use the notation

$$\kappa = \exp\left(\operatorname{sign}(q) \int_0^{L^e} \theta^e(s)\, ds\right).$$

We have

$$\lim_{q\to 0} \overline{\rho}^e(\rho, q) \;=\; \lim_{q\to 0} \frac{|q|}{a} \sqrt{-W_{-1}\left(-\frac{1}{\eta(\rho,\, q)} \exp(-\frac{1}{\eta(\rho,\, q)})\, \kappa\right)} \tag{47}$$

$$= \rho \lim_{q\to 0} \frac{1}{\frac{1}{\sqrt{\eta(\rho,\, q)}}} \sqrt{-W_{-1}\left(-\frac{1}{\eta(\rho,\, q)} \exp(-\frac{1}{\eta(\rho,\, q)})\, \kappa\right)} \tag{48}$$

Moreover, we have $\lim_{q\to 0} \frac{1}{\eta(\rho,\, q)} = \infty$. With (15) l'Hospital's rules yield

$$\begin{aligned}
&\lim_{\xi\to\infty} \frac{-W_{-1}\left(-\xi \exp(-\xi)\, \kappa\right)}{\xi} \\
=\; &\lim_{\xi\to\infty} \frac{-W_{-1}\left(-\xi \exp(-\xi)\, \kappa\right)}{-\xi \exp(-\xi)\, \kappa \left[1 + W_{-1}\left(-\xi \exp(-\xi)\, \kappa\right)\right]} (\xi - 1) \exp(-\xi)\, \kappa \\
=\; &\lim_{\xi\to\infty} \frac{\xi - 1}{\xi} = 1.
\end{aligned}$$

Now with (48) with the choice $\xi = \frac{1}{\eta}$ we obtain (44). In order to prove (45) we consider the equations

$$\lim_{q\to 0} \overline{\rho}^e(\rho_0,\, q) = \rho_0 \qquad \text{and} \qquad \lim_{q\to 0} \eta(\overline{\rho}^e(\rho_0,\, q),\, q) = \eta(\rho_0,\, q). \tag{49}$$

With the notation $\rho^e(L^e) = \overline{\rho}^e(\rho_0,\, q)$, $\eta_0 = \eta(\rho_0,\, q)$, $\eta_L = \eta(\overline{\rho}^e(\rho_0,\, q),\, q)$ from (32) we get

$$\lim_{q\to 0} \partial_\rho \overline{\rho}^e(\rho_0,\, q) = \lim_{q\to 0} \frac{\rho_0}{\overline{\rho}^e(\rho_0,\, q)} \frac{1 - \eta_0}{1 - \eta_L]} = 1$$

which yields (45). Furthermore, in order to prove (46), from (33) we get for $q \neq 0$

$$\partial_q \overline{\rho}^e(\rho_0,\, q) \;=\; -\operatorname{sign}(q) \frac{1}{a\sqrt{\eta_L}} \left[\frac{\frac{\eta_L}{\eta_0} - 1}{1 - \eta_L}\right] = -\frac{\operatorname{sign}(q)}{a} \left[\frac{\frac{\sqrt{\eta_L}}{\eta_0} - \frac{1}{\sqrt{\eta_L}}}{1 - \eta_L}\right].$$

We have

$$\frac{\sqrt{\eta_L}}{\eta_0} - \frac{1}{\sqrt{\eta_L}} \;=\; a\, \frac{1}{\overline{\rho}^e(\rho_0,\, q)} \left(\frac{\rho_0^2 - \overline{\rho}^e(\rho_0,\, q)^2}{|q|}\right).$$

Now we consider the corresponding limit. We get

$$\lim_{q\to 0} \frac{\rho_0^2 - \overline{\rho}^e(\rho_0,\, q)^2}{|q|}$$

$$
\begin{aligned}
&= \lim_{q\to 0} \frac{1}{|q|}\left[\rho_0^2 + \frac{|q|^2}{a^2} W_{-1}\left(-\frac{1}{\eta(\rho_0,\, q)}\, \exp(-\frac{1}{\eta(\rho_0,\, q)})\, \kappa\right)\right] \\
&= \lim_{q\to 0} \frac{1}{a\,\rho_0\,\sqrt{\eta(\rho_0,\, q)}}\left[\rho_0^2 + \eta(\rho_0,\, q)\,\rho_0^2\, W_{-1}\left(-\frac{1}{\eta(\rho_0,\, q)}\, \exp(-\frac{1}{\eta(\rho_0,\, q)})\, \kappa\right)\right] \\
&= \lim_{\xi\to\infty} \frac{1}{a\,\rho_0}\, \sqrt{\xi}\rho_0^2\left[1 + \frac{1}{\xi}\, W_{-1}\left(-\xi\, \exp(-\xi)\, \kappa\right)\right] \\
&= \lim_{\xi\to\infty} \frac{\rho_0}{a}\, \left[\frac{\xi + \, W_{-1}\left(-\xi\, \exp(-\xi)\, \kappa\right)}{\sqrt{\xi}}\right] \\
&= \lim_{\xi\to\infty} \frac{\rho_0}{a}\, \left[\frac{1 + \, \frac{1-\xi}{\xi}}{\frac{1}{2\,\sqrt{\xi}}}\right] = 0.
\end{aligned}
$$

From (50) this yields the first equality in (46). The other equation in (46) has already been stated in Lemma 3.6. Thus we have proved Lemma 4.2. □

In the next lemma we give the flow rate q^e for a subsonic stationary flow through the pipe corresponding to the edge e if at both end points of the pipe suitable values for the densities are prescribed, that is values that are sufficiently close to each other.

Lemma 4.3. *Let $e = (v, w) \in E$, $\rho^v > 0$, $\rho^w > 0$, $L^e > 0$ and $\theta^e > 0$ be given. Assume that if $\rho^v \neq \rho^w$ the distance $|\rho^v - \rho^w|$ is sufficiently small in the sense that we have*

$$
\frac{\min\{(\rho^v)^2,\, (\rho^w)^2\}}{(\rho^w)^2 - (\rho^v)^2}\, \left[2\,\ln\left(\frac{\rho^w}{\rho^v}\right) - \operatorname{sign}(\rho^v - \rho^w)\, \int_0^{L^e} \theta^e(s)\, ds\right] > 1. \tag{50}
$$

The solution q^e of the equation

$$
\rho^w = \overline{\rho}^e(\rho^v, q^e) \tag{51}
$$

is given by the equation $q^e = 0$ if $\rho^v = \rho^w$. If $\rho^v \neq \rho^w$, a we get a subsonic stationary flow with

$$
\begin{aligned}
\operatorname{sign}(q^e) &= \operatorname{sign}(\rho^v - \rho^w), &(52)\\
|q^e| &= a\,\sqrt{\frac{(\rho^w)^2 - (\rho^v)^2}{2\,\ln\left(\frac{\rho^w}{\rho^v}\right) - \operatorname{sign}(q^e)\, \int_0^{L^e} \theta^e(s)\, ds}}. &(53)
\end{aligned}
$$

Proof. If $\rho^v = \rho^w$, $q^e = 0$ solves equation (51).

So let us assume in the sequel that $\rho^v \neq \rho^w$. With the definition (23) of the function $\overline{\rho}^e$, for η as defined in (22), (51) implies the equation

$$
\frac{\eta(\rho^v,\, q^e)}{\eta(\rho^w,\, q^e)} = \exp\left(\frac{1}{\eta(\rho^w,\, q^e)} - \frac{1}{\eta(\rho^v,\, q^e)}\right)\, \exp(\operatorname{sign}(q^e)\, \int_0^{L^e} \theta^e(s)\, ds). \tag{54}
$$

This yields

$$
\frac{(\rho^w)^2}{(\rho^v)^2} = \exp\left(a^2\, \frac{(\rho^w)^2 - (\rho^v)^2}{(q^e)^2}\right)\, \exp(\operatorname{sign}(q^e)\, \int_0^{L^e} \theta^e(s)\, ds). \tag{55}
$$

This is in turn equivalent to equation (53).

If $\rho^v > \rho^w$, since $\overline{\rho}^e$ is decreasing with respect to q^e we have $q^e > 0$. On the other hand, if $\rho^v < \rho^w$ this yields $q^e < 0$, and (52) follows.

Inequality (50) implies that we have $\frac{1}{\eta} = \frac{a^2 \min\{(\rho^v)^2, (\rho^w)^2\}}{(q^e)^2} > 1$ that is the flow is subsonic. Thus we have shown Lemma 4.3. □

Lemma 4.3 motivates the definition of the function

$$\overline{q}^e(\rho^v, \rho^w) = \begin{cases} \operatorname{sign}(\rho^v - \rho^w)\, a \sqrt{\frac{(\rho^v)^2 - (\rho^w)^2}{2\ln\left(\frac{\rho^v}{\rho^w}\right) + \operatorname{sign}(\rho^v - \rho^w) \int_0^{L^e} \theta^e(s)\, ds}} & \text{if} \quad \rho^v \neq \rho^w, \\ 0 \quad \text{if} \quad \rho^v = \rho^w \end{cases} \tag{56}$$

that is $\overline{q}^e(\rho^v, \rho^w)$ is defined as the solution of (51). Note that $\overline{q}^e$ is strictly increasing with respect to ρ^v and strictly decreasing with respect to ρ^w.

The following lemma presents a representation of the function $\overline{q}^e$ that is more suitable for the construction of the stationary states on the network.

Corollary 1. *For $\rho^w > 0$, with*

$$\zeta = \frac{\rho^v}{\rho^w} > 0$$

we can write $\overline{q}^e$ in the form $\overline{q}^e(\rho^v, \rho^w) = Q^e(\zeta, \rho^w)$ with

$$Q^e(\zeta, \rho^w) = \begin{cases} \rho^w \operatorname{sign}(\zeta - 1)\, a \sqrt{\frac{\zeta^2 - 1}{2\ln(\zeta) + \operatorname{sign}(\zeta - 1) \int_0^{L^e} \theta^e(s)\, ds}} & \text{if} \quad \zeta \neq 1, \\ 0 \quad \text{if} \quad \zeta = 1. \end{cases} \tag{57}$$

Then Q^e is continuous and strictly increasing with respect to ζ and with respect to ρ^w. For $\zeta \neq 1$, Q^e is continuously differentiable.

In order get unique subsonic stationary states on the graph depicted in Figure 6 for $q_0 > 0$ and $\rho_0 > 0$ with

$$\frac{q_0}{\rho_0} < a$$

we introduce some auxiliary functions. For our arguments the monotonicity properties of these auxiliary function are essential.

From the given boundary data, the density at the vertex b_0 is determined to be

$$\rho^b = \overline{\rho}^{e_1}(\rho_0, q_0) \tag{58}$$

and the flow rate is $q_1 = q_0$. For a real number $q_2 \in [0, q_1]$ define the functions

$$\begin{aligned} \rho^e(q_2) &= \overline{\rho}^{e_2}(\rho^b, q_2) \\ \rho^f(q_2) &= \overline{\rho}^{e_3}(\rho^b, q_1 - q_2), \\ q_4(q_2) &= \overline{q}^{e_4}(\rho^e(q_2), \rho^f(q_2)). \end{aligned}$$

By Lemma 3.6 and Lemma 4.2, ρ^e is strictly decreasing and ρ^f is strictly increasing. With Corollary 1 this implies that q_4 is strictly decreasing. Now we define the auxiliary function

$$\beta(q_2) = \overline{\rho}^{e_5}(\rho^e(q_2), q_2 - q_4(q_2)) - \overline{\rho}^{e_6}(\rho^f(q_2), q_1 - q_2 + q_4(q_2)). \tag{59}$$

Remark 3. The function value of β is a measure for the violation of the node condition (42) at c_0 with the flow that is generated with $q_2 = q^*$ as defined in (60) below. The equation $\beta(q^*) = 0$ holds if and only if (42) holds at c_0. In this case, $q_2 = q^*$ generates a classical subsonic stationary state on the whole network.

We have $\rho^e(0) = \rho^b$, $\rho^f(0) = \overline{\rho}^{e_3}(\rho^b, q_1) < \rho^b$, $q_4(0) = \overline{q}^{e_4}(\rho^b, \rho^f(0)) > 0$. Hence we have

$$\beta(0) = \overline{\rho}(\rho^b, -q_4(0), L_5, \theta_5) - \overline{\rho}(\rho^f(q_2), q_1 + q_4(0), L_6, \theta_6) > \rho^b - \rho^b = 0.$$

On the other hand we have $\rho^e(q_1) < \rho^b$, $\rho^f(q_1) = \rho^b$, $q_4(q_1) < 0$. Hence we have

$$\beta(q_1) = \overline{\rho}^{e_5}(\rho^e(q_1),\, q_1 - q_4(q_2)) - \overline{\rho}^{e_6}(\rho^b,\, q_4(q_2)) < \rho^b - \rho^b = 0.$$

The monotonicity properties stated above imply that β is strictly decreasing. Moreover, β is continuous on the interval $[0,\, q_1]$. Thus Bolzano's intermediate value theorem implies that there exists a unique value $q_* \in (0,\, q_1)$ such that $\beta(q_*) = 0$. If we extend the domain of β, the extended function (that is well-defined as long as a subsonic state exists) is still decreasing, hence for subsonic flows with $q > q_1$ we get $\beta(q) \leq \beta(q_1) < 0$ and for $q < 0$ we get $\beta(q) \geq \beta(0) > 0$. Hence no feasible flow exists outside of $(0,\, q_1)$.

Using q_*, we get a stationary state as follows: We define the feasible flow

$$\begin{pmatrix} q_1 \\ q_2 \\ q_3 \\ q_4 \\ q_5 \\ q_6 \\ q_7 \end{pmatrix} = \begin{pmatrix} q_0 \\ q_* \\ q_0 - q_* \\ q_4(q_*) \\ q_* - q_4(q_*) \\ q_0 - q_* + q_4(q_*) \\ q_0 \end{pmatrix} \in Q \tag{60}$$

that satisfies (43) at the junctions b_0, c_0, e_0 and f_0. We define the densities

$$\begin{pmatrix} \rho^a \\ \rho^b \\ \rho^c \\ \rho^d \\ \rho^e \\ \rho^f \end{pmatrix} = \begin{pmatrix} \rho_0 \\ \rho^b \\ \overline{\rho}^{e_5}(\rho^e(q_*), q_* - q_4(q_*)) \\ \overline{\rho}^{e_7}(\rho^c, q_0) \\ \rho^e(q_*) \\ \rho^f(q_*) \end{pmatrix}$$

with ρ^b as defined in (58). Then the densities satisfy (42) at the junctions b_0, c_0, e_0 and f_0, since $\beta(q_*) = 0$ implies

$$\rho^c = \overline{\rho}^{e_6}(\rho^f(q_*), q_0 - q_* + q_4(q_*)).$$

Thus we have shown that also for the diamond graph in Figure 6 a unique subsonic stationary state exist for suitable given boundary values ρ_0 and q_0. This result is summarized in the following Theorem:

Theorem 4.4. *Let a network with 7 horizontal pipes of the structure shown in Figure 6 with the corresponding pipe data (lengths and values of θ^e) be given be given. Let the density $\rho_0 > 0$ at a_0 and the flow rate $q_0 > 0$ at d_0 be given. Assume that ρ_0 is sufficiently large in the sense that for the squared Mach number η_0 we have*

$$\eta_0 = \frac{q_0^2}{a^2(\rho_0)^2} < 1$$

and the length L^{e_1} satisfies $L^{e_1} < x_c(\eta_0)$, with x_c as defined in (26). Let ρ^b as in (58) denote the density at b_0. Assume that for the remaining pipes, for all the paths that connect b_0 and d_0, classical subsonic stationary states exist for the density ρ^b at b_0 and the flow rate q_0.

Then on the network there exists a unique classical subsonic stationary state with constant flow rates along each pipe that satisfies (18) on each pipe and the node conditions (42) and (43) at the junctions b_0, c_0, e_0 and f_0.

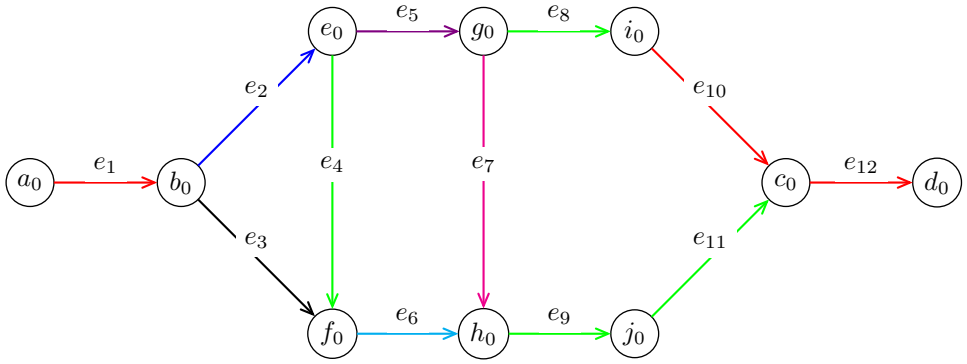

FIGURE 7. A graph with a circle with 2 parallel chords

Remark 4. For the computation of the stationary state, we can consider the problem to find a root of the function β defined in (59). By the definition of β, this requires the computation of the functions $\overline{\rho}$ and $\overline{q}$ as defined in (23), (56).

Example 5. If $\int_0^{L^{e_2}} \theta^{e_2}(s)\,ds = \int_0^{L^{e_3}} \theta^{e_3}(s)\,ds$ and $\int_0^{L^{e_5}} \theta^{e_5}(s)\,ds = \int_0^{L^{e_6}} \theta^{e_6}(s)\,ds$ we have $\overline{\rho}^{e_2} = \overline{\rho}^{e_3}$ and $\overline{\rho}^{e_5} = \overline{\rho}^{e_6}$ and thus $q_* = \frac{1}{2}q_0$ and $q_4 = 0$.

Similar as in Section 4.1, by induction we can generalize this result to the case of a graph that contains a circle with N parallel chords. For the case of $N = 2$ parallel chords, we can depict the graph as in Figure 7.

The graph consists of the V-shaped part $G_V = (V_V, E_V)$ with the vertices $V_V = \{a_0, b_0, e_0, f_0\}$ and the edges $\{e_1, e_2, e_3\}$, a finite number of graphs that contain the chords and the junction part that is for the case $N = 2$ from Figure 7 given by $G_J = (V_J, E_J)$ with $V_J = \{i_0, j_0, c_0, d_0\}$, $E_J = \{e_{10}, e_{11}, e_{12}\}$ that are glued together.

Again we assume that the density $\rho_0 > 0$ and the flow rate $q_0 > 0$ at the input node are given. In order to avoid technicalities, in the derivation of the classical subsonic stationary states, we assume that ρ_0 is sufficiently large such that throughout the construction, only subsonic flows occur in the network (that is, the values of $\int_0^{L^e} \theta^e(s)\,ds$ for the pipes are sufficiently small).

For the construction of the stationary state, we start again as in the case of the graph from Figure 6 (that is with $N = 1$ chord). At the bifurcation at b_0 the gas flow is determined by the parameter q_2 that describes how the flow is distributed. As in the derivation of Lemma 4.4, we consider the graph $G_1 = (V_1, E_1)$ with $V_1 = \{a_0, b_0, e_0, f_0, g_0, h_0\}$, $E_1 = \{e_1, e_2, e_3, e_4, e_5, e_6\}$. In this graph each value of $q_2 \in [0, q_1]$ for the distribution of the flow at b_0 generates a state with the given inflow q_0 and the given density ρ_0 at a_0 where in general the generated density values at the vertices g_0 and h_0 will not be equal.

The induction argument works as follows: Suppose that for the graph that consists of the first bifurcation G_V and is extended such that it contains the edges of the N parallel chords, the data at the output nodes are known as a function of the parameter $q_2 \in [0, q_1]$ that determines the distribution of the flow at b_0. We call the upper output node (for $N = 1$ this is g_0) e_N^l and the lower output node (for $N = 1$ this is h_0) e_N^r. We make the following *induction assumption* that holds for $N = 1$ by the derivation of Lemma 4.4:

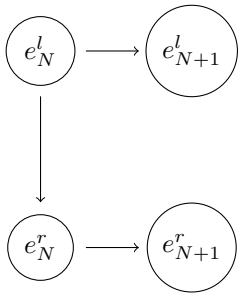

FIGURE 8. The notation for the vertices at the right-hand side of the graph with $(N+1)$ parallel chords.

The functions $\rho^{e_N^l}(q_2)$, $\rho^{e_N^r}(q_2)$ *are known and continuous and* $\rho^{e_N^l}$ *is strictly decreasing,* $\rho^{e_N^r}$ *is strictly increasing. Moreover, we assume that the corresponding flow rates* $q^{e_N^l}(q_2)$, $q^{e_N^r}(q_2)$ *are known and continuous and* $q^{e_N^l}$ *is strictly increasing,* $q^{e_N^r}$ *is strictly decreasing. Moreover we assume the inequalities*

$$q^{e_N^l}(0) < 0 \tag{61}$$
$$q^{e_N^r}(0) > q_1 \tag{62}$$
$$\rho^{e_N^l}(0) > \rho^{e_N^r}(0) \tag{63}$$
$$q^{e_N^l}(q_1) > q_1 \tag{64}$$
$$q^{e_N^r}(q_1) < 0 \tag{65}$$
$$\rho^{e_N^l}(q_1) < \rho^{e_N^r}(q_1). \tag{66}$$

The interpretation of (61) in terms of the flow for $N = 1$ is that if $q_2 = 0$, that is the complete flow is lead through e_3, then there is a suction effect at g_0 since the flow through e_4 is strictly positive. Hence at h_0, not only q_1 but also the flow that enters at g_0 and passes through e_4 arrives, which implies (62). So in this situation we have a flow from g_0 to h_0. Since the gas flows from points with higher density values to points with lower density values, this implies (63). The assumptions (64), (65), (66) can be interpreted analogously.

In the induction step to obtain the graph with $N+1$ parallel chords the next parallel chord is glued to the output nodes of the given graph with N parallel chords.

For example, for the step from $N = 1$ to 2 we go from the graph G_1 to the graph $G_2 = (V_2, E_2)$ where with $V_2 = \{a_0, b_0, e_0, f_0, g_0, h_0, i_0, j_0\}$, $E_2 = \{e_1, e_2, e_3, e_4, e_5, e_6, e_7, e_8, e_9\}$. Using the functions $\overline{\rho}$ and $\overline{q}$, we can give an explicit representation of the flow through the resulting graph.

Figure 8 shows the notation for the vertices at the right-hand side of the graph with $(N+1)$ parallel chords. We have

$$\rho^{e_{N+1}^l}(q_2) = \overline{\rho}^{(e_N^l, e_{N+1}^l)}(\rho^{e_N^l}(q_2),\, q^{e_N^l}(q_2) - \overline{q}^{(e_N^l, e_N^r)}(\rho^{e_N^l}(q_2),\, \rho^{e_N^r}(q_2))).$$

Note that $\rho^{e_{N+1}^l}(q_2)$ is strictly decreasing. Analogously we have

$$\rho^{e_{N+1}^r}(q_2) = \overline{\rho}^{(e_N^r, e_{N+1}^r)}(\rho^{e_N^r}(q_2),\, q^{e_N^r}(q_2) + \overline{q}^{(e_N^l, e_N^r)}(\rho^{e_N^l}(q_2),\, \rho^{e_N^r}(q_2)))$$

and $\rho^{e_{N+1}^r}(q_2)$ is strictly increasing. Now we define the function

$$\beta^{N+1}(q_2) = \rho^{e_{N+1}^l}(q_2) - \rho^{e_{N+1}^r}(q_2).$$

Then β^{N+1} is strictly decreasing.

Due to (63), (61) and (62) we have

$$q^{e^l_{N+1}}(0) < 0 \quad \text{and } q^{e^r_{N+1}}(0) > q_1. \tag{67}$$

Moreover we get

$$\rho^{e^l_{N+1}}(0) > \rho^{e^r_{N+1}}(0). \tag{68}$$

This implies

$$\beta^{N+1}(0) > 0.$$

Moreover, we have shown that for $N+1$ our induction assumptions (63), (61) and (62) hold. Due to (66), (64) and (65) we have

$$q^{e^l_{N+1}}(q_1) > q_1 \quad \text{and } q^{e^r_{N+1}}(q_1) < 0. \tag{69}$$

Hence we get

$$\rho^{e^l_{N+1}}(q_1) < \rho^{e^r_{N+1}}(q_1). \tag{70}$$

This implies

$$\beta^{N+1}(q_1) < 0.$$

Moreover, we have shown that for $N+1$ our induction assumptions (66), (64) and (65) hold.

By induction, this implies that for all N the function β^N has a unique root q^* in the interval $[0, q_1]$. Moreover, since β is decreasing, there cannot exist a root that corresponds to a subsonic state outside the interval $[0, q_1]$.

If the vertices e^l_{N+1} and e^r_{N+1} are now identified to the edge c_0 (that is in the case $N = 2$, i_0 and j_0 are identified with c_0, that is the edges e_{10} and e_{11} vanish as edges of length zero), this value of q^* determines the unique subsonic stationary flow through the graph with a circle and N chords that do not intersect.

5. **Stationary states for sloped pipes.** In this section we consider the case of pipes with nonzero slopes $z^e \neq 0$. This case is of particular importance for pipelines that transport gas over mountains. In this section we assume that θ^e and z^e are constant.

First we consider the case $q^e = 0$. Then for ρ^e the stationary states are determined by the ordinary differential equation

$$a^2 \, (\rho^e)_x = -(\rho^e) \, g z^e.$$

This yields the density

$$\rho^e(x) = \rho^e(0) \, \exp(-\frac{g \, z^e}{a^2} \, x). \tag{71}$$

In the sequel we assume that $q \neq 0$. We define the number

$$c_0^e = \frac{2 \, g \, z^e}{a^2 \, \theta^e \, \mathrm{sign}(q^e)}.$$

Define the interval

$$I_{c_0^e} \quad = \quad \begin{cases} (0, \ 1), & \text{if} \quad c_0^e > 0; \\ (-c_0^e, \ 1), & \text{if} \quad c_0^e \in (-1, \ 0). \end{cases}$$

For $\tau \in I_{c_0^e}$ define the auxiliary function

$$F_{c_0^e}(\tau) = \frac{1}{c_0} \left((1 + c_0^e) \, \ln(|c_0^e + \tau|) - \ \ln(\tau) \right).$$

Then $F_{c_0^e}$ is differentiable and for the derivative

$$F'_{c_0^e}(\tau) = \frac{\tau - 1}{\tau(\tau + c_0^e)}$$

we have $F'_{c_0^e}(\tau) < 0$, thus $F_{c_0^e}$ is strictly decreasing on $I_{c_0^e}$. The second derivative is

$$F''_{c_0^e}(\tau) = \frac{-\tau^2 + 2\,\tau + c_0}{\tau^2(\tau + c_0^e)^2}$$

For $c_0^e > -1$ and $\tau \in I_{c_0^e}$ we have $F''_{c_0^e}(\tau) > 0$, thus $F_{c_0^e}$ is convex.

With the function $F_{c_0^e}$, we can write the differential equation (4) in the form of the differential equation (7) with $d_0 = \theta^e \operatorname{sign}(q^e)$. Due to Lemma 3.1 for $\eta^e(0) \in I_{c_0^e}$ we can represent the solution in the form

$$\eta^e(x) = F^{-1}_{c_0^e}\left(F_{c_0^e}(\eta_0) - \ \theta^e \operatorname{sign}(q^e)\ x\right). \tag{72}$$

If c_0^e is a rational number, $c_0^e = \frac{m}{n}$ with integers n and m, with the notation $f = F_{c_0^e}(\tau)$ the number $\tau = F^{-1}_{c_0^e}(f)$ is a solution of the equation

$$\exp(m\ f)\ \tau^n - \left|\frac{m}{n} + \tau\right|^{n+m} = 0.$$

Example 6. For $c_0^e = -\frac{1}{2}$ this yields

$$F^{-1}_{c_0^e}(f) = \frac{1}{2}\ \mathrm{e}^f\ \left(1 - \sqrt{1 - 2\mathrm{e}^{-f}}\right) = \frac{1}{1 + \sqrt{1 - 2\mathrm{e}^{-f}}}.$$

Observe that $F^{-1}_{c_0^e}(f)$ is defined for $f \in (\ln(2), \infty)$ and is decreasing from 1 to $\frac{1}{2}$.

Since $F'_{c_0^e}(1) = 0$, For $q^e > 0$, Lemma 3.3 implies that there is a critical length $x_c > 0$ where the state becomes sonic and there is a blow up in the derivative ρ_x. Hence at this point the stationary state breaks down as a classical solution. For $q^e < 0$, this follows from Lemma 3.4.

Analogously to Lemma 3.6, we can derive the sensitivities of the stationary states with respect to q^e and $\rho^e(0)$.

Lemma 5.1. *Assume that a subsonic classical stationary solution exists on $[0, L^e]$. For subsonic states with $q^e \neq 0$ and $\eta^e(0) \in I_{c_0^e}$ we have the partial derivatives*

$$\partial_{\rho^e(0)}\rho^e(L^e) \ = \ \frac{F'_{c_0^e}(\eta^e(0))}{F'_{c_0^e}(\eta^e(L^e))} > 0, \tag{73}$$

$$\partial_{q^e}\rho^e(L^e) \ = \ \frac{\rho^e(L^e)}{q^e}\left(1 - \frac{\eta^e(0)}{\eta^e(L^e)}\ \frac{F'_{c_0^e}(\eta^e(0))}{F'_{c_0^e}(\eta^e(L^e))}\right) < 0. \tag{74}$$

In particular, $\rho^e(L^e)$ is strictly increasing as a function of $\rho^e(0)$ for a fixed value of q^e. Moreover, $\rho^e(L^e)$ is strictly decreasing as a function of q^e.

If $q^e = 0$, we have $\rho^e(L^e) = \rho^e(0)\ \exp(-\frac{g\,z^e}{a^2}\ L^e)$. Thus for $q^e = 0$, we have

$$\partial_{\rho^e(0)}\rho^e(L^e)|_{q^e=0} = \exp(-\frac{g\,z^e}{a^2}\ L^e)$$

and also in this case $\rho^e(L^e)$ is strictly increasing as a function of $\rho^e(0)$.

Proof. Let x and $x_0 \in [0, L^e]$ be given. By (2) again we get

$$\partial_{\rho^e(x_0)}\rho^e(x) \ = \ \frac{|q^e|}{a}\ \left(-\frac{1}{2}\frac{1}{(\eta^e(x))^{3/2}}\right)\ \partial_{\eta^e(x_0)}\eta^e(x)\ \partial_{\rho^e(x_0)}\eta^e(x_0). \tag{75}$$

We have $\partial_{\rho^e(x_0)}\eta^e(x_0) = -2\frac{(q^e)^2}{a^2\,\rho^e(x_0)^3}$ and (9) yields

$$\partial_{\eta^e(x_0)}\eta^e(x) \quad = \quad \frac{F'_{c_0^e}(\eta^e(x_0))}{F'_{c_0^e}(\eta^e(x))} \tag{76}$$

With the choice $x_0 = 0$ and $x = L^e$ inserting (76) in (75) yields (73).

By (2) again we get

$$\partial_{q^e}\rho^e(x) \quad = \quad \frac{\operatorname{sign}(q^e)}{a\sqrt{\eta^e(x)}} - \frac{|q^e|}{2\,a\,(\eta^e(x))^{3/2}}\,\partial_{\eta^e(x_0)}\eta^e(x)\,\partial_q\eta^e(x_0). \tag{77}$$

We have $\partial_q\eta^e(x_0) = \frac{2\,q^e}{a^2\,\rho^e(x_0)^2}$ and inserting (76) in (77) yields (74) with the choice $x_0 = 0$ and $x = L^e$. The fact that the auxiliary function $H_{c_0^e}(\tau) = \tau\,F'_{c_0^e}(\tau) < 0$ is strictly increasing implies that the partial derivative in (74) is negative. □

5.1. **The case $\eta^e(0) < -c_0^e$.** As already stated, for $\eta^e(0) = -c_0^e$, the differential equation (5) has the constant solution (6) and for $\eta^e(0) = 0$ it has the constant solution zero. Now we consider the case where $c_0^e < 0$ and $\eta^e(0) \in (0,1)$ satisfies $\eta^e(0) < -c_0^e$. In this case the corresponding trajectories are caught between the two constant solutions. Define the interval

$$I_0 = (0,\,1) \cap (0,\,-c_0^e).$$

For $\tau \in I_0$ we have $F'_{c_0^e}(\tau) > 0$. Therefore in contrast to the case that we have considered in the previous section for $\eta^e(0) \in I_0$ we define $d_0 = -\theta^e \operatorname{sign}(q^e)$ and for $\tau \in I_0$ we set $F_-(\tau) = -F_{c_0^e}(\tau)$. Then we have $F'_-(\tau) < 0$, and with the function F_-, for $\eta^e(0) \in I_0$ we can write the differential equation (5) in the form of the differential equation (7) and the assumptions of Lemma 3.1 hold. Thus we can represent the solution in the form (72)

Note that (5) implies that in this case η^e is strictly decreasing for $q^e > 0$.

If c_0^e is a rational number, $c_0^e = \frac{m}{n}$ with integers n and m, with the notation $f = F_-(\tau)$ the number $\tau = F_-^{-1}(f) \in I_0$ is a solution of the equation

$$\exp(-m\,f)\,\tau^n - \left|\frac{m}{n} + \tau\right|^{n+m} = 0.$$

Example 7. For $c_0^e = -\frac{1}{2}$ this yields

$$F_-^{-1}(f) = \frac{1}{1+\sqrt{1+2\mathrm{e}^f}}.$$

Observe that for negative values of f, $F_{c_0^e}^{-1}(f)$ is close to $\frac{1}{2}$ and decreases rapidly around zero to values close to 0 that are attained on the positive half-axis. In particular, F_-^{-1} is neither convex nor concave. Note that in this example where $c_0^e \in (-1,0)$, the solution of (5) for $\eta^e(0) \in I_0$ exists on the whole real line.

The representations of the partial derivatives that we have given in (73) and (74) from Lemma 5.1 hold also for the case that we consider in this section since

$$\frac{F'_{c_0^e}(\eta^e(0))}{F'_{c_0^e}(\eta^e(L^e))} = \frac{F'_-(\eta^e(0))}{F'_-(\eta^e(L^e))}.$$

In particular, $\rho^e(L^e)$ is strictly increasing as a function of $\rho^e(0)$ for a fixed value of q^e, since also in this case we have $\partial_{\rho^e(0)}\rho^e(L^e) > 0$. In order to analyse the sign of

the partial derivative with respect to q^e, also in this case we consider the auxiliary function $H_{c_0^e}(\tau) = \tau\, F'_{c_0^e}(\tau) > 0$. For the derivative of $H_{c_0^e}$ we have

$$H'_{c_0^e}(\tau) = \frac{1 + c_0^e}{(\tau + c_0^e)^2} > 0 \tag{78}$$

for $c_0^e > -1$, thus $H_{c_0^e}$ is strictly increasing. Therefore as in (74) for $c_0^e > -1$ we get $\partial_{q^e}\rho^e(L^e) < 0$, hence $\rho^e(L^e)$ is strictly decreasing as a function of q^e.

We summarize our results in stating that for all $e \in E$, both for the case of horizontal pipes where $z^e = 0$ that we have discussed in Section 3.2 and in the case of sloped pipes for $c_0^e > -1$ where $z^e \neq 0$ that is discussed in Section 5, the value $\rho^e(L^e)$ is strictly decreasing as a function of q^e for a fixed value of $\rho^e(0)$. Moreover, for a fixed value of q^e the value $\rho^e(L^e)$ is strictly increasing as a function of $\rho^e(0)$.

6. **Outlook.** In this paper we have shown how subsonic classical stationary states for the isothermal Euler equations can be constructed for certain networks that can contain an arbitrary number of circles. We have also shown that the stationary states are uniquely determined by the prescribed boundary values.

The construction of the states has shown that in many case, for example for horizontal pipes, if the input pressure is too low, the stationary state breaks down as a classical solution at some point in the pipes (the critical length) where the Mach number converges to one, that is the state is sonic. For the purpose of gas transport, such a state is not suitable. Sound speed is much to fast for the transportation of gas because pipe vibrations can occur that can damage the system and cause noise pollution. From the mathematical point of view, the stationary solution can be continued over the critical length by considering a weaker notion of solutions, where a singularity in the derivative is allowed. For a discussion of such solutions see [6].

Our construction of classical stationary solutions on networks of horizontal pipes with circles has also clarified that due to the continuity of the density, reversed flow in parallel pipes cannot occur. In fact nonzero circular flows do not satisfy the node conditions. If we follow a nonzero circular flow, then along the circle, the density values are strictly decreasing, thus there cannot be a continuity of the density in the circle.

In the future, we want to generalize the construction of stationary states to obtain a method that works for networks that have a structure that is given by an arbitrary graph. Moreover, the questions of exact controllability between stationary states and stabilization are of interest. The control action in the system is driven by compressors that are located in the interior of the network, see [13, 14].

The stabilization of the flow in fan–shaped graph has already been investigated in [11]. For more general graphs, as in [11], the existence of classical solutions in a C^1–neighborhood of the stationary states can be shown using Theorem 2.1 in [16]. In order to show the exponential decay of the system with linear Riemann feedback, a network Lyapunov function of the type that is defined in [11] can be used. This Lyapunov function is an extension of the Lyapunov function introduced in [8] by Coron, d'Andrea-Novel and Bastin.

REFERENCES

[1] M. K. Banda, M. Herty and A. Klar, Coupling conditions for gas networks governed by the isothermal Euler equations, *Networks and Heterogenous Media,* **1** (2006), 295–314.

[2] A. Bressan, S. Canic, M. Garavello, M. Herty and B. Piccoli, Flows on networks: recent results and perspectives, *EMS Reviews in Mathematical Sciences,* **1** (2014), 47–111.
[3] R. Carvalho, L. Buzna, F. Bono, M. Masera, D. K. Arrowsmith and D. Helbing, Resilience of natural gas networks during conflicts, crises and disruptions, *PLOS ONE,* **9** (2014), e0090265.
[4] F. Chapeau-Blondeau, Numerical evaluation of the lambert W function and application to generation of generalized Gaussian noise with exponent 1/2, *IEEE Transactions on Signal Processing*, **50** (2002), 2160–2165.
[5] R. M. Colombo and F. Marcellini, Smooth and discontinuous junctions in the p-system, *Journal of Mathematical Analysis and Applications,* **361** (2010), 440–456.
[6] R. M. Colombo, G. Guerra, M. Herty and V. Schleper, Optimal control in networks of pipes and canals, *SIAM J. Control Optim.*, **48** (2009), 2032–2050.
[7] R. M. Corless, G. H. Gonnet, D. E. G. Hare, D. J. Jeffrey and D. E. Knuth, On the Lambert W function, *Adv. Comp. Math.,* **5** (1996), 329–359.
[8] J.-M. Coron, B. d'Andrea-Novel and G. Bastin, A strict Lyapunov function for boundary control of hyperbolic systems of conservation laws, *IEEE Trans. Automat. Control,* **52** (2007), 2–11.
[9] M. Dick, M. Gugat and G. Leugering, Classical solutions and feedback stabilization for the gas flow in a sequence of pipes, *Networks and Heterogeneous Media,* **5** (2010), 691–709.
[10] M. Garavello and B. Piccoli, Conservation laws on complex networks, *Annales de l'Institut Henri Poincare (C) Non Linear Analysis,* **26** (2009), 1925–1951.
[11] M. Gugat, M. Dick and G. Leugering, Gas flow in fan-shaped networks: Classical solutions and feedback stabilization, *SIAM Journal on Control and Optimization,* **49** (2011), 2101–2117.
[12] M. Gugat and M. Herty, Existence of classical solutions and feedback stabilization for the flow in gas networks, *ESAIM: Control, Optimisation and Calculus of Variations,* **17** (2011), 28–51.
[13] M. Gugat, M. Herty and V. Schleper, Flow control in gas networks: Exact controllability to a given demand, *Mathematical Methods in the Applied Sciences,* **34** (2011), 745–757.
[14] M. Herty, Modeling, simulation and optimization of gas networks with compressors, *Networks and Heterogeneous Media,* **2** (2007), 81–97.
[15] J. H. Lambert, Observationes variae in mathesin puram, *Acta Helvetica, physico-mathematico-anatomico-botanico-medica,* **3** (1758), 128–168.
[16] T. Li, B. Rao and Z. Wang, Exact boundary controllability and observability for first order quasilinear hyperbolic systems with a kind of nonlocal boundary conditions, *Discrete Contin. Dyn. Syst.,* **28** (2010), 243–257.
[17] A. Martin, M. Möller and S. Moritz, Mixed integer models for the stationary case of gas network optimization, *Mathematical Programming*, **105** (2005), 563–582.
[18] G. A. Reigstad, Numerical network models and entropy principles for isothermal junction flow, *Networks and Heterogeneous Media,* **9** (2014), 65–95.
[19] V. Schleper, M. Gugat, M. Herty, A. Klar and G. Leugering, Well-posedness of networked hyperbolic systems of balance laws, in *Constrained Optimization and Optimal Control for Partial Differential Equations,* International Series of Numerical Mathematics, 160, Birkhäuser/Springer Basel AG, Basel, 2012, 123–146.
[20] D. Veberic, *Having fun with Lambert W(x) function*, arXiv:1003.1628
[21] G. P. Zou, N. Cheraghi and F. Taheri, Fluid-induced vibration of composite natural gas pipelines, *International Journal of Solids and Structures*, **42** (2005), 1253–1268.

Received September 2014; revised December 2014.

E-mail address: martin.gugat@fau.de
E-mail address: markus.hirsch-dick@fau.de
E-mail address: hante@math.fau.de
E-mail address: leugering@math.fau.de